# $\alpha$- and $\beta$-Crystalline Forms of Isotactic Polypropylene Investigated by Nanoindentation

**THOMAS LABOUR, LAURENT FERRY, CATHERINE GAUTHIER, PHILIPPE HAJJI, GÉRARD VIGIER**

Groupe d'Etudes de Métallurgie Physique et de Physique des Matériaux, UMR-CNRS 5510, Institut National des Sciences Appliquées, Bâtiment 502, 20 Avenue Einstein, 69621 Villeurbanne Cedex, France

*Received 13 October 1998; accepted 27 February 1999*

**ABSTRACT:** Under special crystallization conditions from the melt, both $\alpha$- and $\beta$-forms of isotactic polypropylene were produced simultaneously. The $\alpha$- and $\beta$-spherulites of polypropylene were differentiated under optical microscope, allowing the nanoindentation of individual spherulites of each crystallographic form. Elastic modulus and hardness of $\beta$-spherulites were found to be 10 and 15% respectively lower than in $\alpha$-spherulites. The higher stiffness of $\alpha$ may be related to the particular interlocked structure with cross-hatched lamellae, and to a lower molecular mobility in the crystallites. © 1999 John Wiley & Sons, Inc. J Appl Polym Sci 74: 195–200, 1999

**Key words:** polypropylene; spherulites; $\beta$-form; nanoindentation

## INTRODUCTION

Isotactic polypropylene (PP) is known to display at least three different crystalline forms, namely the monoclinic $\alpha$-form, the hexagonal $\beta$-form, and the triclinic $\gamma$-form.[1–3] In the melt crystallized PP, essentially the $\alpha$-form is produced. The microstructure and mechanical properties of the $\alpha$-form PP have been investigated intensively.[1–6] In contrast, little information is available on the mechanical behavior of the $\beta$-form PP. The $\beta$-form occurs only occasionally and at levels of only a few percent, the $\beta$-spherulites developing sporadically in the melt at high undercooling. Under special crystallization conditions or when selective $\beta$-nucleators are used, higher levels of $\beta$-form can be produced.[4] Recently, it has been found that high purity $\beta$-form PP exhibits lower values of elastic modulus and yield stress.[5,6] However, to date, no measurement of elastic properties has been performed on pure $\beta$-form PP, free of $\beta$-nucleating agents, since $\beta$-form always coexists with nonnegligible amounts of $\alpha$-form.

The present article aims to compare the elastoplastic properties of a $\beta$-spherulite to those of an $\alpha$-spherulite. Nanoindentation is a particularly well-suited technique to determine the mechanical behavior of very small volumes of matter. Close indents can be processed with a high spatial resolution, and a small indentation depth combined to a high resolution enables accurate measurement of the local properties on the inside of individual spherulites. Subsequently, Young's modulus and hardness could be determined for both $\alpha$- and $\beta$-spherulites.

## EXPERIMENTAL

### Materials

The polypropylene used in this work was manufactured by Solvay Bruxelle (ELTEX PHV001P). This commercial grade contains 0.2 wt % antioxidant stabilizer and has a melt flow rate of 10 (ASTM D-1238).

Correspondence to: G. Vigier.

Journal of Applied Polymer Science, Vol. 74, 195–200 (1999)
 CCC 0021-8995/99/010195-06

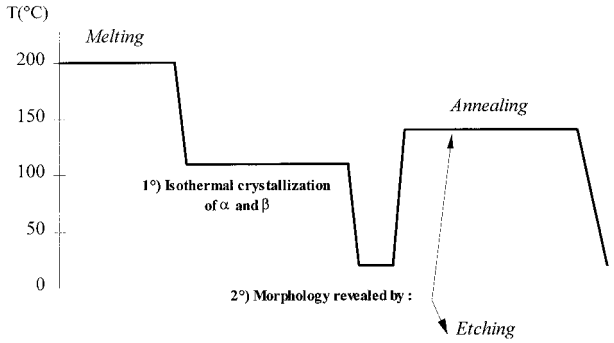


**Figure 1** Thermal program of crystallization and subsequent annealing to reveal the spherulitic morphology.

Pellets of the polymer were pressed into a molded plate by a compression press heater at 180°C under a pressure of 350 bars for 2 min, after a preheating at 180°C under 1 bar for 1 min. The moulded plate, 4 mm thick, was quenched by a cold press at 25°C under 35 MPa. The cooling time was ~200 s.

### *Thermal Program Producing β-Form*

This nanoindentation study requires the crystallization of $\beta$-spherulites, which occurs under special time-temperature conditions. By performing slow cooling from the melt, only the $\alpha$-form is crystallized. Homogeneous nucleation of $\alpha$ proceeds at higher temperatures as compared with $\beta$: 115–135°C and 105–125°C, respectively. Thus, the growth of $\alpha$-spherulites may fill up the sample before $\beta$ is nucleated. This early invasion of $\alpha$-spherulites is prevented by a rapid cooling from the melt. Consequently, $\beta$-form can only develop if isothermal crystallization is carried out at adequate *Tc* temperature: within the nucleation range of $\beta$.

Plates (25 mm × 14 mm) were cut out of the molded material and encapsulated in an aluminum frame 0.2 mm thick. The samples were heated up to 200°C, held for 20 min to remove previous thermal history, then suddenly immersed in a silicon oil bath maintained at *Tc* = 110°C. The materials were kept in the bath for 30 min, then quenched into cold water (Figure 1).

Relative amounts of $\beta$-form were found to reach the highest level of 10%, as determined by considering the empirical ratio, *k,* extracted from wide angle X-ray scattering (WAXS) pattern.[2]

### *Sample Preparation for Microscopy Observation of α- and β-Spherulites*

Spherulites of $\alpha$- and $\beta$-form can easily be differentiated after acid etching, and then separately indented. However, etching is believed to modify strongly the surface of the sample, and thus to affect the accuracy of measurement.

In the course of this study, an alternative treatment, assumed to be less detrimental, was developed which allows revealing of the spherulitic structure while leaving the mark of the indents unaffected. By performing this annealing treatment after indentation of the bulk sample, each value could be related to the crystallographic form ($\alpha$ or $\beta$) of the spherulite, in which indentation had been processed.

The face of the sample chosen for nanoindentation was first progressively abrased with several different emery papers, and then polished with a very fine diamond paste (1 $\mu$m) until no residual scratches were visible. To bring the spherulitic morphology into relief, two methods denoted "permanganic etching" and "annealing" have been used.

### *Permanganic Etching*

The sample was immersed for 6 h in an acid solution consisting of 1.3 wt % $KMnO_4$/32.9 wt % $H_3PO_4$/65.8 wt % concentrated $H_2SO_4$. The permanganic solution etches mainly the amorphous part of the polymer and consequently the lamellar organization in the spherulites will be revealed.[7] The crystalline structures of individual spherulites are easily differentiated through direct observation with a standard optical microscope since the $\alpha$-spherulites appear with a bright contrast whereas the $\beta$-spherulites exhibit a dark aspect (Figure 2).

### *Annealing*

Isothermal crystallization at large undercooling is supposed to give rise to high thermal stress concentrations between spherulites. Moreover, the most unstable microstructure is known to be located at the spherulitic boundaries. Upon annealing, these boundaries undergo substantial transformations: thermal stresses are able to relax, stresses may rise from differential thermal expansion between $\alpha$ and $\beta$, and unstable lamellae may recrystallize. All these mechanisms may change the surface topography of the spherulitic boundaries and bring them into relief, as was observed in our experiments.

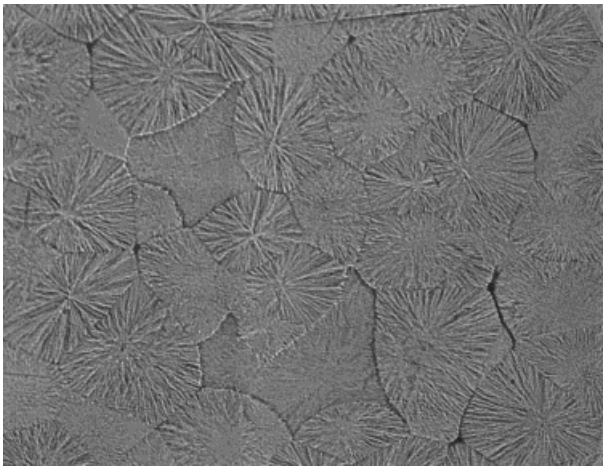

**Figure 2** Optical micrograph after chemical etching, showing predominant bright α-spherulites and dark β-spherulites.

The sample was annealed in an oven at 140°C for 30 min and cooled to room temperature (at approximately −30°C/min). Optical microscopy was performed on the specimens without further modification. Objects were observed in reflected and polarized light. The spherulite boundaries were revealed and the crystalline structures of individual spherulites were differentiated easily in examining their contrast and their surface characteristics: α-spherulites have a bright aspect, a smooth surface, and a convex shape, whereas β-spherulites appear with a dark contrast, a rough surface, and a concave shape.

## TECHNIQUE

The results were obtained by using a Nano Indenter II™ from Nano Instruments Inc. (Knoxville, TN), a special hardness tester capable of measuring continuous load, $P$, and displacement, $h$, during indentation tests, with resolutions close to 75 nN and 0.04 nm. This apparatus consists of three major components: the indenter, an optical microscope, and a precision table that transports the specimen between the microscope and the indenter.[8]

First, the position of at least one indent is selected on the specimen surface using the optical microscope part. The fact that the position of the indentation can be determined to 0.5 μm means that this technique can be used to probe small volumes of material and thus permits an access to local properties. Nevertheless, all measurements must be made sufficiently far apart from each other, to avoid the overlapping of the plastically deformed zones that exist around indents.

A specific indentation procedure involving several loading, unloading, and holding segments, was used at a speed of 10 nm/s until a fixed depth of 500 nm and ended by complete unloading at the same speed.[9] A typical load-displacement curve, *P-h,* showing the first loading and the last unloading steps is presented in Figure 3. Under loading, the indentation depth, $h_{max}$, is the superposition of an elastic component, $h_e$, and a plastic one, $h_p$:

$$h_{max} = h_e + h_p \tag{1}$$

The plastic component, $h_p$, which corresponds to the residual deformation, is the intercept of the unloading curve with the depth axis.

The local hardness, $H$, and the Young's modulus, $E$, of the specimen are given by the following equations[10–13]:

$$H = \frac{P_{max}}{A} \tag{2}$$

$$E_r = \frac{\sqrt{\pi}}{2} \cdot \frac{S}{\sqrt{A}} \tag{3}$$

$$\frac{1}{E_r} = \frac{1 - \nu^2}{E} + \frac{1 - \nu_i^2}{E_i} \tag{4}$$

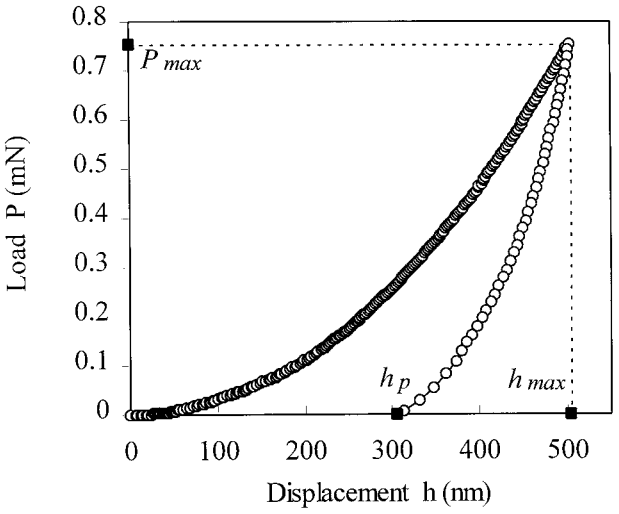


**Figure 3** Load-displacement curve of indentation (loading and unloading steps).

**Table I Elastic Modulus and Hardness of α- and β-Spherulites, Obtained from Different Testing Procedures**

| | $E$ (α-Spherulite) | | $E$ (β-Spherulite) | | $H$ (α-Spherulite) | | $H$ (β-Spherulite) | |
|---|---|---|---|---|---|---|---|---|
| Procedure | Mean (GPa) | SD | Mean (GPa) | SD | Mean (MPa) | SD | Mean (MPa) | SD |
| Etching *before* indentation | 2.72 | 0.17 | 2.47 | 0.18 | 124 | 21 | 100 | 8 |
| Annealing *before* indentation | 2.59 | 0.12 | 2.28 | 0.09 | 118 | 14 | 97 | 7 |
| Annealing *after* indentation | 2.63 | 0.11 | 2.43 | 0.17 | 110 | 8 | 97 | 12 |

where $P_{max}$ is the maximum load applied onto the sample before unloading (i.e., when $h = h_{max}$), $E_r$ is the "reduced modulus," $\nu$ is the Poisson ratio of the tested material, $\nu_i$ and $E_i$ are the Poisson ratio and the Young's modulus of the indenter tip, respectively, $S$ is the contact stiffness as determined by the slope of the tangent to the $P$-$h$ unloading curve at $P = P_{max}$, and finally, $A$ is the contact area between the indenter tip and the material under the maximum load $P_{max}$. $A$ is estimated from the knowledge of (i) the contact depth, $h_c$, and (ii) a function which describes the shape of the indenter tip from this contact depth.[8]

In the present study, the value of $\nu = 0.3$ has been chosen for PP but it should be noted that the Poisson ratio value has no influence on the calculated hardness and only a small one on the calculated modulus (e.g., using $\nu = 0.38$ instead of $\nu = 0.30$ gives a modulus variation below 6%).

## RESULTS

### Indentation after Acid Etching

In Table I, Young's modulus $E$ and hardness $H$, measured on spherulites revealed with various techniques, are reported. Because acid etching provides a remarkable selectivity, this technique was used at first to reveal the spherulitic structure of PP. One α-spherulite and one β-spherulite were selected; 10 indents were performed in each. The values of $E$ were taken to be the mean of the 10 values for each series. The β-form exhibits a nearly 10% lower modulus than the α-form. The same trend of lower rigidity is observed for the hardness, and even increased, the hardness of β-form appearing 15% lower than α-form. Nevertheless, acid etching is known to affect strongly the surface of the sample, and consequently may introduce uncertainty, since both crystalline forms are surely modified in a different manner. This can partly explain the high standard deviations of the results that make it difficult to really conclude. A supposed smoother way of revealing the spherulitic structure was then performed.

### Indentation after Annealing

Annealing was performed to make the spherulite boundaries observable, then the same indentation procedure was followed to test individual spherulites of α- or β-form. The temperature and the time at annealing temperature (140°C for 30 min) were chosen sufficiently low in order that the microstructure and thus the elastic properties were not affected by lamellar thickening, perfection of the lamellae or recrystallization, as was verified considering the melting endotherm of the specimen in differential scanning calorimetry (DSC). Very similar results as with etching were obtained. This indicates that the perturbation introduced by etching on the sample surface is mainly the same for both α- and β-spherulites. On an absolute basis, the values registered after annealing appear generally lower than after etching. However, the values appear to depend significantly on the technique used to reveal the microstructure. The results were obtained on samples chemically or thermally modified prior to nanoindentation. A special procedure was developed to avoid this preliminary stage, ensuring that the trends observed are conclusive.

### Indentation before Annealing

The specimen that was only polished is first indented. Two hundred fifty-six regularly spaced indents (each 25 μm) are performed inside a square zone of 375 μm × 375 μm. Then, the specimen is annealed at 140°C (Figure 4). The residual marks of the indents and the spherulitic structure are visible simultaneously. Thus, each registered value can be attributed to α- or β-form.

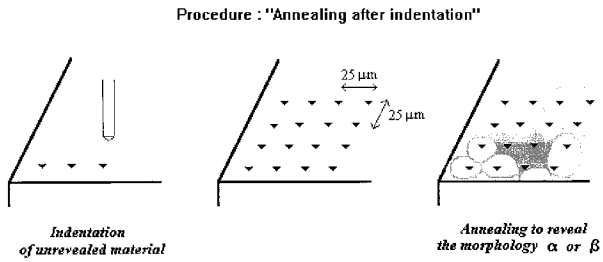


**Figure 4** Schematic procedure to visualize simultaneously the marks of the indents and the spherulitic morphology.

This method is thought to produce the most conclusive way to determine $E$ and $H$ in relation to crystalline form. β-Form exhibits a lower modulus than α-form: 2.43 GPa and 2.63 GPa, respectively. Correspondingly, the hardness of β-form is lower than that of α-form: 96.7 MPa and 110.0 MPa, respectively. The standard deviations calculated for both crystalline forms are small enough to conclude on the separation of both distributions.

Despite high standard deviations of the results, especially when performing etching before nanoindentation, the three techniques used to reveal the spherulitic structure lead to the same conclusion: the β-spherulites exhibit lower modulus and hardness than α ones.

Performing the indentation before the microstructure was revealed is the most reliable procedure and can be taken as a reference to determine which effect other revealing techniques had on the surface of the specimen. Acid etching appears to introduce a small hardening effect, while annealing has a marked softening effect, probably due to the relaxation of thermal stresses generated during crystallization of the sample.

## DISCUSSION

Generally speaking, variations of intraspherulitic elastic properties in a semicrystalline polymer may be due to changes of its microstructural characteristics: percent crystallinity, lamellar thickness, intercrystalline tie molecules, and lamellar arrangement.

Pure samples of α- and β-form were found to have nearly the same percent crystallinity.[3] Thus, we can assume that spherulites of each form have the same proportion of crystalline and amorphous phase.

Lamellar thickness and density of tie molecules may affect the elastic modulus to some extent. At constant percent crystallinity, the smaller the crystallite size (which generally implies more tie molecules), the higher the modulus.[14] Recently, the lamellar thickness of PP has been observed directly by scanning force microscopy (SFM).[15] It appears that lamellae of β-form are slightly thicker than the radial and the tangential lamellae of α-form.

In contrast, many reports assume that β-form exhibit more interlamellar tie chains than α-form, due to a higher crystallization growth rate.[3,6] This better coupling would lead to a higher modulus.

Anyway, the leading contributing factor toward contrasting elastic properties of α and β seems to be mostly their different lamellar arrangements. Authors have pointed out that the simpler lamellar morphology of β ("sheaf-like" structure) should be less rigid than the radial arrangement of α.[6] The β-spherulites consist of parallel-stacked lamellae, tending to pack into bundles. On the other hand, the α-spherulites consist of an aggregate of lamellae that radiate from the central nucleus outward.

Moreover, when the α-form is crystallized at high undercooling, a secondary set of crystallites grows along the tangential direction of the spherulites in the interstices between the radial crystallites.[16–18] The presence of tangential crystallites in α-spherulites, building a rigid "cross-hatched" network, makes the deformation of the amorphous component in the intercrystalline zone much more difficult.[19] Therefore, this interlocked structure stiffens considerably the α-spherulites, and explains the significantly lower modulus of β-form depicted in our measurements.

The β-form that displays a lower hardness seems to be more ductile than the α-form. The same structural differences evoked to explain the modulus variations could be responsible for the hardness ones. Particularly, the presence of tangential crystallites in α-spherulites limits the lamellar separation.[19] Thus, the aforementioned interlocked structure of α-spherulites is thought to delay the plastic deformation, while maintaining the elastic response up to high stress levels: the yield stress and thus the hardness are increased.

Furthermore, the relative decrease in hardness appears even higher than the relative decrease in modulus. This could be due to a different molecular mobility in the crystallites of α and β, leading

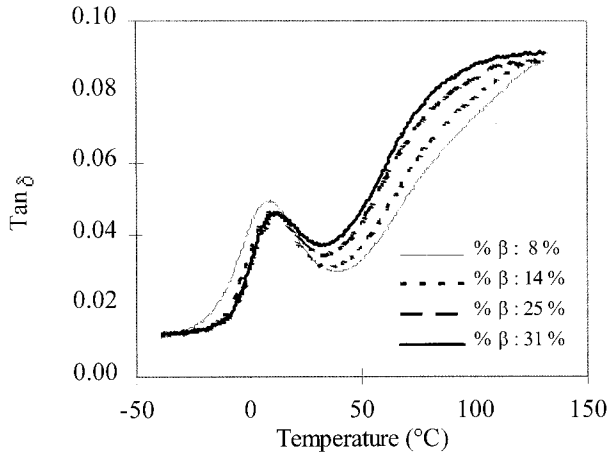


**Figure 5** Dynamic mechanical loss factor (tan δ) versus temperature for specimens containing various amounts of β-form (at constant overall percent crystallinity, mean lamellar thickness, and mean spherulite size).

to a different deformability. It was reported that the high-temperature relaxation peak is shifted with increasing β-form content toward lower temperatures.[3,6]

We found the same trend in PP filled with stearate coated calcium carbonate, on specimens with various amounts of β-form, while keeping all other crystalline characteristics (overall percent crystallinity, lamellar thickness, spherulite size) identical[20] (Figure 5). The filler was introduced at a constant fraction of 10 vol % to produce higher levels of β-form and induced no direct modification of the high-temperature relaxation process.

As this relaxation is thought to be the consequence of long-distance stress-assisted diffusion of crystallographic defects,[21] this shift would mean that the molecular mobility within the crystallites is higher in the β-form compared with the α-form; the plastic glide becomes easier, giving rise to a lower hardness.

## CONCLUSIONS

Nanoindentation was performed on individual spherulites of α- or β-form. A procedure was developed to avoid the detrimental effect of etching on measurements. The β-spherulites exhibit a lower modulus and a lower hardness than the α-spherulites. This behavior was assigned to structural differences between both phases in the arrangement of the lamellae and in the molecular mobility within the crystallites.

The authors thank Dr. G. Orange and Dr. Y. Bomal, of Rhodia Recherches (C.R.A., Aubervilliers, France) for support in this research, and the Management of Rhodia for permission to publish this work.

## REFERENCES

1. Padden, F. J.; Keith, H. D. J Appl Phys 1959, 30, 1479.
2. Turner-Jones, A.; Aizlewood, J. M.; Beckett, D. R. Makromol Chem 1964, 75, 134.
3. Jacoby, P.; Bersted, B. H.; Kissel, W. J.; Smith, C. E. J Polym Sci, Part B 1986, 24, 461.
4. Shi, G.; Zhang, X.; Cao, Y.; Hong, J. Makromol Chem 1993, 194, 269.
5. Karger-Kocsis, J.; Varga, J. J Appl Polym Sci 1996, 62, 291.
6. Tjong, S. C.; Shen, J. S.; Li, R. K. Y. Polym Eng Sci 1996, 36, 100.
7. Olley, R. H.; Bassett, D. C. Polymer 1982, 23, 1707.
8. Oliver, W. C.; Pharr, G. M. J Mater Res 1992, 7, 1564.
9. Hajji, P.; Ferry, L.; Labour, T.; Vigier, G. to appear.
10. Tabor, D. Proc R Soc, A 1948, 192, 247.
11. Ternovskii, A. P.; Alekhin, V. P.; Shorshorov, M. K. H.; Khrushchov, M. M.; Skvortsov, V. N. Zavod Lab 1973, 39, 1242.
12. Bulychev, S. I.; Alekhin, V. P.; Shorshorov, M. K. H.; Ternovskii, A. P.; Shnyrev, G. D. Zavod Lab 1975, 41, 1137.
13. Bulychev, S. I.; Alekhin, V. P. Zavod Lab 1987, 53, 76.
14. Nielsen, L. E.; Stockton, F. D. J Polym Sci, Part A 1963, 1, 1995.
15. Castelein, G.; Coulon, G.; Aboulfaraj, M.; G'Sell, C.; Lepleux, E. J Phys III (France) 1995, 5, 547.
16. Bassett, D. C.; Olley, R. H. Polymer 1984, 25, 935.
17. Norton, D. R.; Keller, A. Polymer 1985, 26, 704.
18. Olley, R. H.; Bassett, D. C. Polymer 1989, 30, 399.
19. Aboulfaraj, M.; G'Sell, C.; Ulrich, B.; Dahoun, A. Polymer 1995, 36, 731.
20. Labour, T.; Gauthier, C.; Vigier, G.; Orange, G.; Bomal, Y. to appear.
21. Jourdan, C.; Cavaille, J. Y.; Perez, J. J Polym Sci, Part B 1989, 27, 2361.